Phys. Lett. B 878 (2026) 140503

Contents lists available at ScienceDirect

Physics Letters B

journal homepage: www.elsevier.com/locate/physletb

Letter

Does the electron EDM preclude electroweak baryogenesis?

Yuan-Zhen Li [a,b,c,*], Michael J. Ramsey-Musolf [d,e,f,g], Jiang-Hao Yu [a,b,h,i,j]

[a] CAS Key Laboratory of Theoretical Physics, Institute of Theoretical Physics, Chinese Academy of Sciences, Beijing, 100190, China
[b] School of Physical Sciences, University of Chinese Academy of Sciences, Beijing, 100049, PR China
[c] Centre for Cosmology, Particle Physics and Phenomenology, Université catholique de Louvain, Louvain-la-Neuve, B-1348, Belgium
[d] Tsung-Dao Lee Institute & School of Physics and Astronomy, Shanghai Jiao Tong University, Shanghai, 200240, China
[e] Shanghai Key Laboratory for Particle Physics and Cosmology, Key Laboratory for Particle Astrophysics and Cosmology (MOE), Shanghai Jiao Tong University, Shanghai, 200240, China
[f] Amherst Center for Fundamental Interactions, Department of Physics, University of Massachusetts, Amherst, MA 01003, USA
[g] Kellogg Radiation Laboratory, California Institute of Technology, Pasadena, CA, 91125, USA
[h] Center for High Energy Physics, Peking University, Beijing, 100871, China
[i] School of Fundamental Physics and Mathematical Sciences, Hangzhou Institute for Advanced Study, UCAS, Hangzhou, 310024, China
[j] International Centre for Theoretical Physics Asia-Pacific, Beijing/Hangzhou, China

ARTICLE INFO

Editor: Prof Ryuichiro Kitano

Keywords:
Electroweak baryogenesis
Electric dipole moment
CP violation
Quantum transport theory

ABSTRACT

Electroweak baryogenesis (EWBG) constitutes a theoretically compelling and experimentally testable mechanism for explaining the origin of the baryon asymmetry of the universe (BAU). New results for the electric dipole moment (EDM) of the electron place significant constraints on the beyond Standard Model CP-violation needed for successful EWBG. Using a specific model illustration, we show how new developments in EWBG quantum transport theory that include CP-violating sources first order in gradients imply more relaxed EDM constraints – and thereby greater EWBG viability – than implied by previous approximation formulations. We also illustrate how these developments enable a more realistic treatment of CP-conserving interactions that can also have a decisive impact on the predicted BAU.

Explaining the origin of the baryon asymmetry of the universe (BAU) is a key unsolved problem at the interface of particle and nuclear physics with cosmology. Both the mechanism for baryogenesis as well as the early universe era in which it occurred remain unknown. A compelling possibility is electroweak baryogenesis (EWBG), which links the BAU to the spontaneous electroweak symmetry breaking (EWSB) and generation of elementary particle masses via the Higgs mechanism [1–3] (For reviews, see *e.g.*, [4–6]). In principle, the Standard Model (SM) of particle physics contains the necessary ingredients for EWBG [7]: B-violation via electroweak (EW) sphaleron processes; C- and CP-violation in the electroweak sector; and out-of-equilibrium conditions in the guise of a first order electroweak phase transition (FOEWPT) to the present Higgs phase. In practice, the latter does not occur for a Higgs boson heavier than $\sim 70-80$ GeV [8–10], while the effects of CP-violation (CPV) in the Cabibbo-Kobayashi-Maskawa (CKM) matrix are too feeble to have generated the observed BAU, even for a sufficiently light Higgs boson [11–13].

Physics beyond the Standard Model (BSM) can remedy these shortcomings. An extended scalar sector can readily lead to a FOEWPT even for a 125 GeV Higgs boson (see [14] for extensive references), while providing the efficient CPV. The requisite mass scale for these new particles ($\lesssim 700$ GeV) as well as the needed strength of their coupling to the Higgs boson generically puts them within the reach of future high energy collider searches and precision Higgs boson studies [14]. Results from the Large Hadron Collider do not preclude such an extended scalar sector, and it may require a future 100 TeV pp collider to provide a definitive test [14]. Next generation gravitational wave detectors, such as LISA, Taiji, and Tianqin, provide a complementary probe and could uncover a stochastic gravitational wave background arising from a FOEWPT [15–17].

Searches for the permanent electric dipole moments (EDMs) of atoms, molecules, and nucleons provide the most powerful probe of the BSM CPV needed for EWBG [18–20]. Theoretically, drawing

* Corresponding author.
E-mail addresses: liyuanzhen@itp.ac.cn, yuanzhen.li@uclouvain.be (Y.-Z. Li), mjrm@sjtu.edu.cn, mjrm@physics.umass.edu (M.J. Ramsey-Musolf), jhyu@itp.ac.cn (J.-H. Yu).

https://doi.org/10.1016/j.physletb.2026.140503
Received 29 December 2025; Received in revised form 23 April 2026; Accepted 29 April 2026
Available online 11 May 2026

quantitative inferences about EWBG viability from EDM search results requires performing robust computations of the early universe CPV dynamics. Here, we report on advances addressing this challenge and the corresponding implications for the EDM-EWBG connection.

The EWBG CPV dynamics occur during a FOEWPT that proceeds via nucleation of bubbles of broken electroweak symmetry, defined by regions of non-vanishing, spacetime varying scalar background fields $\varphi(x)$ (*i.e.*, the Higgs field). CPV-interactions at the bubble walls induce a non-zero density of left-handed SM fermions, n_L, that diffuses into the symmetric phase, biasing EW sphaleron transitions into creation of a net B+L number. The latter diffuses back inside the expanding bubbles, where EWSB quenches the sphalerons and preserves the BAU, assuming a sufficiently strong FOEWPT.

The challenge in computing n_L entails solving – in the presence of $\varphi(x)$ – the quantum transport equations for Greens functions that encode information on particle densities. The mass of any particle that interacts with the $\varphi(x)$ varies with spacetime as it traverses the bubble wall, necessitating a continual re-definition of the mass eigenstates. Previous EWBG computations have employed various approaches to solving these transport dynamics [21–32]. For a given set of CPV parameters, the resulting BAU predictions can vary by an order of magnitude. The most optimistic typically result from the use of the "vev insertion approximation" (VIA) [33–37], whose theoretical consistency has been criticized recently in Refs. [26,38,39]. In the proposed alternative, semiclassical (SC) formulation [26,38], the CPV source terms first arise at second order in gradients with respect to position along the bubble wall profile, leading to a significantly smaller BAU than in the VIA (for a review, see Ref. [23]). As a result, the corresponding viability of EWBG with given EDM limits is significantly suppressed or even precluded, according to the predictions of the SC method. The robustness of the transport theory is therefore a key ingredient for the EWBG-EDM interface.

In what follows, we provide a consistent treatment of the EWBG CPV dynamics including the first-order-in-gradients CPV sources [40,41], as well as robust CP-conserving interactions, which avoids both the VIA inconsistencies and the SC approximations. We demonstrate that despite its theoretical shortcomings, the VIA as employed in earlier work can under-predict the magnitude of the BAU, in contrast to the conclusions drawn from the SC treatments. This enhancement in BAU arises from a consistent treatment of flavor mixing in the presence of a spacetime-varying background field, a feature missed by the SC expansion [26,38]. Consequently, the viability of the EWBG model is significantly enhanced, thereby enlarging the EWBG-consistent parameter space in a given model.

Employing a realistic EWBG model [42,43] for illustration, we solve the Kadanoff-Baym transport equations [44–49] using the vev resummation (VR) framework developed in Refs. [40,41]. (See [41] for a detailed delineation of differences between the VR and SC frameworks.) For a given set of model parameters, the VR result for the BAU can be as large or even a few times larger than the VIA prediction. Consequently, EDM constraints on EWBG can be more relaxed than previously realized. We also provide a realistic, quantitative determination of the dependence of the BAU transport dynamics on model parameters – including those that enter the CP-conserving "collision terms" – a feature that has typically eluded earlier studies. While there remain open challenges pertaining to bubble wall dynamics [50–56], the results reported herein constitute a significant advance for assessing the EWBG-EDM interface. We stress that while we illustrate these effects within a specific scalar extension of the Standard Model, the conclusions are generic for any model involving background field-induced CPV mixing between two species, including those with fermionic sources. In this context, the scalar model we adopt serves as a paradigmatic case study for assessing the EWBG-EDM interface. The resulting relaxation of EDM constraints underscores the importance of EWBG as a continuing primary motivation for the worldwide EDM experimental program.

We introduce general features of the scalar field transport dynamics (see [43]) before describing the model illustration. Consider a model with two complex, electrically neutral scalar fields $H^0_{1,2}$ denoted by the "flavor space" vector $\eta \equiv (H^0_1, H^0_2)$. The two flavor components of η interact with scalar fields $\hat{\phi}_k(x)$, whose classical values $\varphi_k(x)$ define the bubble walls. The η-$\varphi_k(x)$ interactions lead to a mass-squared matrix having the generic form

$$M^2_\eta(x) = \begin{pmatrix} M^2_1(x) & R(x)\, e^{-i\,\alpha(x)} \\ R(x)\, e^{i\,\alpha(x)} & M^2_2(x) \end{pmatrix}, \tag{1}$$

where $M_{1,2}(x)$, $R(x)$, $\alpha(x)$ depend on the model parameters and the spacetime-dependence of the $\varphi_k(x)$.

We solve for the neutral scalar Greens functions by first diagonalizing $M^2_\eta(x)$ at each spacetime point using a unitarity transformation $\hat{\eta} = U(x)\eta$, where the hatted fields correspond to the mass eigenstates with diagonal mass-squared matrix $\hat{m}^2(x)$. Evolution of the mass basis particle (anti-particle) density matrices f_m ($\bar{f}_m$) follows from Schwinger-Dyson (SD) equations for the scalar field Wightman functions $G^<_{ij}(x,y) \equiv \langle \hat{H}^\dagger_j(y)\hat{H}_i(x)\rangle$ and $G^>_{ij}(x,y) \equiv \langle \hat{H}_i(x)\hat{H}^\dagger_j(y)\rangle$, where $i,j \in \{1,2\}$. Following [40,41], we transform to Wigner space co-ordinates $X = (x+y)/2$ and k, the wavenumber associated with the relative co-ordinate $x-y$, and reorganize the corresponding SD equations into the Kadanoff-Baym (KB) constraint and kinetic equations.

Observing that there exists a hierarchy of length scales in the problem facilitates a tractable solution to the KB equations. We define the scale ratios: $\epsilon_w \equiv L_{\rm int}/L_w$, $\epsilon_{\rm coll} \equiv L_{\rm int}/L_{\rm mfp}$, and $\epsilon_{\rm osc} \equiv L_{\rm int}/L_{\rm osc}$, where $L_{\rm int} = |\vec{k}| \sim T^{-1}$ is the de Broglie wavelength with T being the temperature of the plasma; L_w is the wall thickness, which in many models is O$(10/T)$, so that $L_w \gg L_{\rm int}$; $L_{\rm osc}$ is the length scale associated with " flavor" oscillations $H^0_1 \leftrightarrow H^0_2$; and $L_{\rm mfp}$ is the mean free path associated with gauge and scalar field interactions. For the scenarios of interest here, one finds $L_{\rm mfp} \gg L_{\rm int}$ for perturbative values of the couplings, while CPV asymmetries are maximized for $L_w \sim L_{\rm osc}$ in the " thick wall" regime [40]. Thus, one has $\epsilon_{w,{\rm coll,osc}} \ll 1$ in the interesting region.

Expanding the constraint and kinetic equations to orders ϵ^0 and ϵ, respectively, yields the following quantum Boltzmann equations for the density matrices:

$$(u\cdot\partial_X + \vec{F}\cdot\nabla_k) f_m(\vec{k},X) = -\Big[i\omega_k + u\cdot\Sigma, f_m(\vec{k},X)\Big] + C_m[f_m,\bar{f}_m](\vec{k},X) \tag{2a}$$

$$(u\cdot\partial_X + \vec{F}\cdot\nabla_k) \bar{f}_m(\vec{k},X) = +\Big[i\omega_k - u\cdot\Sigma, \bar{f}_m(\vec{k},X)\Big] + C_m[\bar{f}_m,f_m](\vec{k},X) \quad , \tag{2b}$$

where $u^\mu = (1,\vec{v})$; $\vec{v} = \vec{k}/\bar{\omega}_k$; $\bar{\omega}_k = \sqrt{|\vec{k}|^2 + \bar{m}^2(x)}$; $\bar{m}^2 = (M_1^2 + M_2^2)/2$; $\vec{F} = \nabla_X \bar{\omega}_k$; $\omega_k = {\rm diag}\{\omega_{1k},\omega_{2k}\}$; $\omega_{ik} = \sqrt{|\vec{k}|^2 + {M_i}^2(x)}$; $\Sigma^\mu = U^\dagger \partial^\mu U$, and the "collision term" C_m is a functional of the f_m and $\bar{f}_m$.

Note that the terms in the LHS of (2a), (2b) generalize the spacetime derivative and force terms in classical Boltzmann equation. The "force" $\vec{F}$ is associated with the variation of the background fields which contribute to $\bar{m}(x)$. On the RHS, the commutator $-i[\omega_k, f_m]$ ($-i[\omega_k,\bar{f}_m]$) gives rise to (anti-)particle flavor oscillations and is identical in form to what appears in the familiar density matrix formalism for neutrino flavor oscillations. Crucially, the commutators $[u\cdot\Sigma, f_m]$ and $[u\cdot\Sigma,\bar{f}_m]$ encode the CP-violating sources. From the definition of $\Sigma^\mu \equiv U^\dagger\partial^\mu U$, it is evident that these sources are linear in the spacetime gradients of the background fields $(\partial^\mu\theta, \partial^\mu\alpha)$. This stands in contrast to the semiclassical (SC) approximation, where CPV sources typically appear at second order in gradients. Finally, the collision term C_m embodies the effect of all interactions that lead to thermalization in the plasma, chemical equilibrium associated with particle species changing reactions, and diffusion ahead of the advancing bubble wall.

The relative sign difference between the oscillation term and CPV source terms in Eqs. (2a), (2b) leads to a net number density (a.k.a.,

CPV asymmetry) for a given particle species. Writing

$$U = \begin{pmatrix} \cos\theta(x) & -\sin\theta(x)e^{-i\alpha(x)} \\ \sin\theta(x)e^{i\alpha(x)} & \cos\theta(x) \end{pmatrix} \tag{3}$$

gives $\Sigma^\mu =$

$$\begin{pmatrix} 0 & e^{-i\alpha} \\ e^{i\alpha} & 0 \end{pmatrix}\partial^\mu\theta + \frac{i}{2}\begin{pmatrix} 2\sin^2\theta & \sin 2\theta e^{-i\alpha} \\ \sin 2\theta e^{i\alpha} & -2\sin^2\theta \end{pmatrix}\partial^\mu\alpha.$$

Combining the first two terms on the RHS of Eqs. (2b), (2b) leads, *e.g.*, for the $(1,1)$ element

$$\left(u\cdot\partial_X + \vec{F}\cdot\vec{\nabla}\right)f_{11} \supset -\left[\, i(\omega_k + \sin^2\theta\, u\cdot\partial\alpha), f\,\right]_{11} + \cdots$$
$$\left(u\cdot\partial_X + \vec{F}\cdot\vec{\nabla}\right)\bar{f}_{11} \supset \left[\, i(\omega_k - \sin^2\theta\, u\cdot\partial\alpha), \bar{f}\,\right]_{11} + \cdots$$

The simultaneous presence of flavor mixing ($\sin\theta \neq 0$) and a spacetime dependent phase ($\partial^\mu\alpha \neq 0$) thus leads to a difference in the particle and antiparticle oscillation frequencies proportional to $\sin^2\theta u\cdot\partial\alpha$ and to a corresponding, non-vanishing CPV asymmetry, $f_{11} - \bar{f}_{11}$.

To illustrate the impact of this effect using the VR framework, we solve Eqs. (2a), (2b) for the "Two-Step EWBG" model of Refs. [42,43]. Baryogenesis occurs during the first of two successive electroweak symmetry-breaking (EWSB) transitions, wherein the $\varphi_k(x) \neq 0$ while the components of η admit no non-vanishing background field values. For renormalizable η-$\hat{\phi}_k$ interactions, the emergence of a spacetime varying phase $\alpha(x)$ in Eq. (1) during the first step requires the presence of at least two non-vanishing $\varphi_k(x)$ [43]. Thus, one requires at least four scalar fields: the two components of η and the two $\hat{\phi}_k$.

A minimal realization entails a scalar sector consisting of two Higgs doublets $H_{1,2}$, a hypercharge $Y = 0$ real triplet Σ, and a SM gauge singlet S. All scalars are $SU(3)_C$ singlets. The gauge and fermion sectors are unchanged from the SM. To model the impact of the latter, we introduce an additional scalar field A, whose dynamics implement all other flavor-diagonal thermalizing interactions in the plasma, such as those arising from gauge and Yukawa interactions. During the first EWSB transition, S and the neutral component of Σ obtain vacuum expectation values (vevs), v_s and v_σ, respectively, with corresponding field flucuations described by $s = S - v_s$ and $\sigma = \Sigma^0 - v_\sigma$. These vevs vary with spacetime, thereby providing the requisite two background fields $\varphi_k(x)$ with $k = 1, 2$. In the second transition, (v_s, v_σ) relax to zero while the neutral components of the doublets obtain vevs, $v_{1,2}$, with $\sqrt{v_1^2 + v_2^2} = 246$ GeV. One may embed the model in a supersymmetric context [57,58], with the corresponding superpartners augmenting the field content. Here we consider the non-supersymmetric version.

For successful EWBG during the first step, this transition must be first order, a condition shown to be satisfied in both perturbative and non-perturbative (lattice) computations for suitable choices of the scalar potential parameters [59,60]. CPV interactions between the $H_{1,2}$ and the (S, Σ) vevs catalyze generation of non-zero Higgs number densities, $n_{H_{1,2}}$. Yukawa interactions then transfer the latter into non-vanishing fermion number densities. The resultant left-handed fermion densities bias electroweak sphalerons into producing a non-zero B+L density that diffuses into the bubble interiors.

The scalar potential is $V(H_1, H_2, \Sigma, S, A) = V_H + V_\phi + V_{H\phi}$, where V_H is the CP-conserving Two Higgs Double Model (2HDM) potential [61–63], V_ϕ involves only the $\phi \equiv (S, \Sigma, A)$ fields, and the key "portal" interaction terms are contained in

$$V_{H\phi} \supset \frac{1}{2}H_1^\dagger H_2\left(a_1 S^2 + a_2\Sigma^2\right) + \text{h.c.}$$
$$+ \sum_{i=1,2}\left[y_1^{ii}S^2 + y_2^{ii}\Sigma^2 + y_3^{ii}A^2\right]H_i^\dagger H_i. \tag{5}$$

The physical (rephasing-invariant) CPV phases are $\delta_S = \arg(a_1^* v_1 v_2^*)$ and $\delta_\Sigma = \arg(a_2^* v_1 v_2^*)$. A combination of these CPV phases and the (S, Σ) vevs induce the $M_i^2(x)$ as well as the $\alpha(x)$ in Eq. (1) and, thus, the CPV sources in the KB equations, as seen in the Supplementary Material. The interactions in Eq. (5) also give rise to Higgs flavor off-diagonal collision terms, which we include in the computation. The A fields do not obtain vacuum expectation values and, thus, do not contribute to the spacetime-dependence in $M_\eta^2(x)$.

To solve Eqs. (2a), (2b) we choose the couplings y_a^{ii} $(a = 1, 2, i = 1, 2)$ so as to yield $\bar{m}^2$ x-independent, implying that $\vec{F} = 0$ in our set up. Doing so allows a direct comparison with the results in Ref. [41]; we will investigate the impact of $\vec{F} \neq 0$ in future work. We then make additional simplifying assumptions relevant to the collision integrals $C_m[f_m, \bar{f}_m]$ outlined in [41,43]. We also consider a type I 2HDM in which only one of the Higgs doublets has Yukawa interactions with the third generation up-type quarks that are in chemical equilibrium. For the interactions of the Higgs particles with the fields A, we assume the corresponding rates Γ_A are large (small) compared to the weak sphaleron and Yukawa (strong sphaleron) interaction rates. We thus obtain $n_L = (4c_T + 5c_Q)n_{H_1}$, where $c_{T,Q}$ are functions of statistical factors k_j relating the number density for a given species n_j to its chemical potential μ_j. In addition, we consider planar bubble walls so that physical quantities depend only on the comoving coordinate $z = X + v_w t$, the distance to the wall, with v_w the wall velocity.

The Higgs number density n_{H_1} is obtained by (i) solving the quantum Boltzmann Eqs. (2a), (2b); (ii) integrating the difference of mass-basis density matrices to obtain the mass-basis number density $\hat{n}$; and (iii) inverting $\eta = U^\dagger\hat{\eta}$ to obtain the flavor basis density for H_1 as $n_{H_1} = \left[U(X)\,\hat{n}(X)\,U(X)^\dagger\right]_{11}$. The baryon number density is then given by

$$n_B = -3\frac{\Gamma_{\rm ws}}{v_w}\int_{-\infty}^{0} dz\, n_L(z)\exp\left(\frac{15}{4}\frac{\Gamma_{\rm ws}}{v_w}z\right), \tag{6}$$

where we have integrated over the region of unbroken EW symmetry in which $\Gamma_{\rm ws}$ is unsuppressed.

To obtain a numerical solution to Eqs. (2a), (2b), which comprise a system of eight coupled integro-differential equations (the f_m and $\bar{f}_m$ are 2×2 matrices in the mass basis), we discretize k and $\cos\theta_k$ into N_k and N_θ bins within the ranges $0 < k < k_{\rm max}$, $-1 < \cos\theta_k < 1$ and take the central values of each bin. The Boltzmann equations then yield a system of $8\times N_k\times N_\theta$ coupled first order ordinary differential equations with boundary conditions, which we solve with the "relaxation method" [64]. Far from the wall, the collision terms bring the density matrices to their equilibrium forms in the positive time direction. Thus, we impose thermal-equilibrium boundary conditions in the negative (positive) time directions for the right-moving (left-moving) modes.

We will compare our results to those obtained in the VIA. The latter framework treats the (S, Σ^0) vevs as perturbative insertions, and otherwise utilizes flavor basis Greens functions. Note that flavor non-diagonal collision terms arising from interactions between the $H_{1,2}$ with s and σ and arising from the first line in Eq. (5), are absent in the VIA treatment. When comparing our results with those of the VIA computation, we follow the methods used in Ref. [43]. For the $v_s(x)$ and $v_\sigma(x)$ profiles we adopt the forms in Ref. [43], along with the corresponding profile parameter values as well as wall velocity, $v_w = 0.05$. The benchmark parameter choices are given in the Supplementary Material.

Fig. 1 shows the resulting VR and VIA profiles $n_L(z)$ as a function of the distance normal to the bubble wall. The pronounced structure near $z = 0$ reflects the variation in the bubble profiles near the wall center and the corresponding impact on the CPV sources involving $u\cdot\Sigma$ entering the RHS of Eqs. (2a), (2b). Importantly, the VR diffusion tail ($z < 0$) is significantly enhanced as compared to the VIA result. As the resulting value of n_B entails integrating over this tail as in Eq. (6) we expect the VR to yield a larger baryon asymmetry.

This expectation is born out as illustrated in Fig. 2 (top), where we show the value of n_B as a function of m_{H_1}. For both the VR and VIA, the increase in n_B for m_{H_1} near m_{H_2} reflects the resonant enhancement as discussed in Refs. [35,40,41]. At the maximum, the VR asymmetry is more than four times larger in magnitude than the VIA value. The double peak structure of VR arises due to a vanishing of the CPV sources

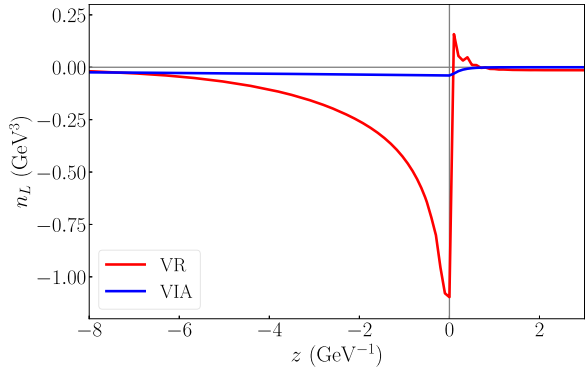

Fig. 1. Left handed quark density $n_L = (4c_T + 5c_Q)n_{H_1}$ for the VIA (blue) and VR (red) approaches. The bubble exterior (interior) corresponds to $z < 0$ ($z > 0$).

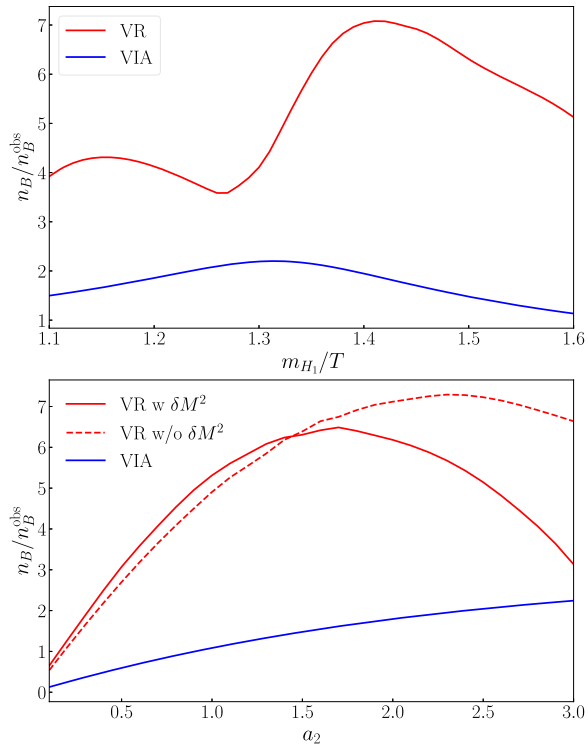

Fig. 2. The obtained BAU n_B as a function of m_{H_1} (with fixed $m_{H_2} = 1.32T$) (top) and the portal coupling a_2 (bottom) for VR and VIA approaches.

$[u \cdot \Sigma, f_m]$ and $[u \cdot \Sigma, \bar{f}_m]$ for $m_{H1} = m_{H2}$ [40]. Thermal mass corrections induce a slight shift in the location of the dip minimum.

The pronounced enhancement of n_B near $m_{H_1} \approx m_{H_2}$ is driven by resonant flavor oscillations. The physical viability of this resonance relies on the interplay between the oscillation frequency, $\Delta\omega_k \equiv |\omega_{1k} - \omega_{2k}|$, and the decoherence induced by plasma interactions. While our VR calculations evaluate the full, coupled integro-differential equations without relying on a simplified damping approximation, we can extract an angle-averaged effective damping rate, $\Gamma_{\rm eff}(k)$, from the linearized off-diagonal collision integrals (see the Supplementary Material for details). Evaluating this rate at the exact location of the resonance peak for a representative momentum $k = T$, we find $\Delta\omega_k/\Gamma_{\rm eff}(k) \approx 2.1$, indicating that the quasiparticle and density-matrix formulations employed in this work remain robust, and off-shell effects are not expected to parametrically alter the predicted BAU. The VR/VIA enhancement away from this degeneracy point is surprising, as earlier work had suggested the VIA significantly over-estimated the asymmetry.

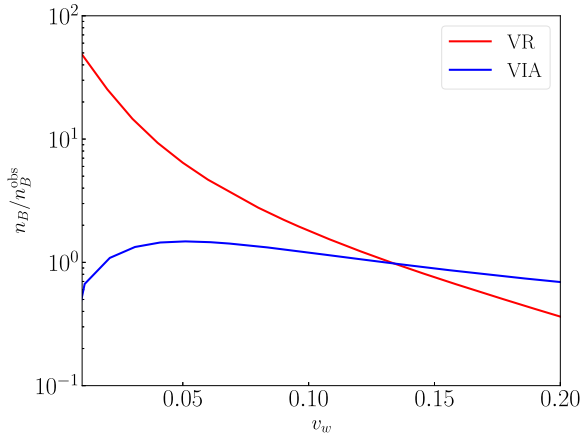

Fig. 3. The obtained BAU n_B as a function of the wall velocity v_w for VR and VIA approaches.

Fig. 2 (bottom) gives the dependence of n_B on the flavor non-diagonal portal coupling a_2, illustrating the impact of flavor non-diagonal interactions that enter the VR treatment via the CPV source and CP-conserving collision term. The VIA includes only the former. Naïvely, one might anticipate increasing $|a_2|$ would lead to a monotonically increasing n_B, owing to correspondingly stronger CPV sources. This expectation is consistent with the VIA curve (blue). In the VR approach, however, for sufficiently large $|a_2|$ the asymmetry begins to decrease, even though the magnitudes of the CPV sources continue to grow. This decrease results from increasingly important damping effects from the CP-conserving collision terms, resulting in closer alignment of the $H_{1,2}$ number densities. An additional suppression at large a_2 arises due to flavor non-diagonal thermal mass corrections in the symmetric phase, δM^2 (dashed red curve). Clearly, a realistic asymmetry computation requires full inclusion and consistent treatment of the CP-conserving interactions, as facilitated by the VR framework.

One can also study the dependence of the resulting BAU on other model parameters, especially the wall velocity v_w, as it affects the BAU through both the particle diffusion and the CP-violating sources. Fig. 3 shows the dependence of the BAU on v_w for both the VR (red) and VIA (blue) approaches, keeping all other benchmark parameters fixed. Typically, the fast-moving wall rapidly sweeps the generated chiral asymmetry into the broken phase, simultaneously decreases the local density $n_L(0)$ and the size of the diffusion tail of $n_L(z)$ ahead of the wall, leaving less time and volume for sphaleron transitions to process the chiral asymmetry. Therefore, increasing v_w generally leads to a smaller BAU. Since effects from the CP-conserving collisions and flavor non-diagonal thermal mass corrections are both neglected in the VIA approach, the BAU predicted by the VIA BAU decreases more slowly with increasing v_w than does the VR BAU. Consequently, the VR approach predicts a significantly larger BAU than the VIA for slow-to-moderate wall velocities ($v_w \lesssim 0.13$), while VIA results may exceed VR results for larger velocities.

In addition, the VIA and VR approaches show distinct behaviors in the slow-wall regime, which is caused by the different wall-velocity dependence of the CPV sources. In the VIA approach, the CPV source is typically proportional to the wall velocity. Consequently, the source vanishes as $v_w \to 0$, causing the sharply dropped BAU. In contrast, the CPV source in the VR framework comes directly from the quantum commutators $[u \cdot \Sigma, f_m]$, which is proportional to the relative velocity of the particles crossing the wall, $v_{\rm rel} = k_z/\omega_k + v_w$. Therefore, the CPV source in the VR approach remains finite as $v_w \to 0$, resulting in a monotonic increasing diffusion tail $n_L(z)$. Furthermore, as $v_w \to 0$, the exponential sphaleron washout factor in Eq. (6) decays infinitely fast for $z < 0$. Consequently, the $1/v_w$ prefactor perfectly cancels with the integral of the washout exponent, and the resulting BAU is strictly dominated by

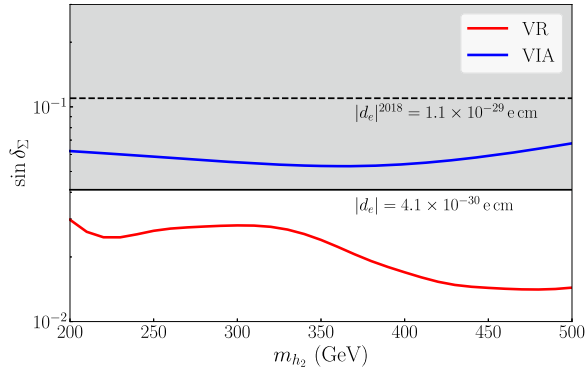

Fig. 4. Constraints on the CPV phase δ_Σ as a function of the physical $T = 0$ mass m_{h_2} with the other parameters fixed. The solid red (blue) band gives the VR (VIA) prediction. The shaded region above the solid (dashed) black line is excluded by the current (previous) electron EDM limit [65,66].

the chiral asymmetry density at the wall boundary, $n_L(0)$. Therefore, the combination of v_w cancellation and a finite CPV source yields the monotonic increase of the BAU at very low velocities in the VR approach.

However, we note that Fig. 3 is plotted starting at $v_w = 0.01$ to reflect the physically valid regime of the EWBG transport framework for both the VR and VIA approaches. Specifically, Eq. (6) intrinsically assumes that the planar bubble wall acts as a sweeping front that eventually overtakes the entire unbroken phase, safely depositing the generated asymmetry into the broken phase where sphalerons are quenched. Mathematically, this sweeping motion is encoded in the lower integration limit of $-\infty$ in Eq. (6), which can be seen as the total spatial reach of the plasma overtaken by the advancing wall. In the extreme limit of an ultra-slow or stationary bubble wall ($v_w \to 0$), this planar wall sweeping approximation physically breaks down, meaning that the swept reach is simply zero and the integration range should collapse to $[0, 0]$. As a result, a static wall would eventually leave all the generated asymmetries in the unbroken phase to be washed out, leading to a vanishing BAU.

In Fig. 4 we show the CPV phase δ_Σ required to generate the observed BAU as a function of m_{h_2}, the physical mass of H_2 at $T = 0$, and compare with the corresponding constraints from experimental limits on d_e. The latter arises in this model from the two-loop "Barr-Zee" graphs [43]. We note that recent studies of general CP-violating Two-Higgs-Doublet Models have demonstrated that alternative two-loop topologies, known as kite diagrams, can yield non-negligible contributions to the electron EDM (see e.g., Ref. [67]). However, in our specific Two-Step EWBG scenario, these kite contributions are analytically zero. Since we assume a CP-conserving 2HDM sector, standard 2HDM kite diagrams contain no CP-violating phase and sum to exactly zero. In addition, the new CP-violating scalar fields (Σ, S) in our scenario lack Yukawa couplings and possess vanishing vacuum expectation values at $T = 0$, therefore they do not mix with the SM-like Higgs doublets and cannot independently form kite topologies. Therefore, the Barr-Zee diagrams evaluated here capture the leading non-vanishing CP-violating effects.

Having made these observations, we find that the present bound $|d_e| < 4.1 \times 10^{-30} e$ cm excludes the shaded region above the solid black line. For reference, we also show the previous d_e bound (dashed black line). The VR and VIA BAU results are indicated by the red and blue lines, respectively. Importantly, according to the VR computation, this EWBG source remains viable even in light of the new d_e bound. In contrast, the VIA computation – and by inference the alternative SC approach – would imply that that model is ruled out.

We stress that application of the VR formulation to other models with either scalar or fermion CPV sources should also yield more relaxed EDM constraints on EWBG than would be inferred from SC and even VIA treatments, thereby enhancing the model's EWBG viability. Indeed, the specific model used herein illustrates the general features of the first-order-in-gradients CPV sources that will apply to any scenario involving flavor mixing between fields interacting with the bubble wall. For fermion sources, the added complexity of spin necessitates inclusion of spin-dependent particle and antiparticle distribution functions; it will not alter the basic feature of a first-order-in-gradients splitting in the corresponding oscillation frequencies. Additionally,the state-of-the art treatment of collision, damping, and flavor oscillation dynamics (both thermal and non-thermal) embodied by the VR framework provides the most realistic treatment of these plasma dynamics achieved to date. This facilitates the resolution of previous inconsistencies between different EWBG CPV dynamic approaches, making the VR framework a realistic approach for confrontation between experiment and any model-specific realization of EWBG.

Data availability

No data was used for the research described in the article.

Declaration of competing interest

The authors declare that they have no known competing financial interests or personal relationships that could have appeared to influence the work reported in this paper.

Acknowledgement

We thank V. Cirigliano, M. Drewes, K. Kainulainen, and K. Ning for helpful discussions. MJRM was supported in part under U.S. Department of Energy contract DE-SC0011095 and the National Natural Science Foundation of China under Grants No. 12375094 and W2441004. JHY and YZL were supported by the National Natural Science Foundation of China under Grants No. 12347105, No. 12375099 and No. 12047503, and the National Key Research and Development Program of China Grant No. 2020YFC2201501, No. 2021YFA0718304.

Supplementary material

Supplementary material associated with this article can be found in the online version at 10.1016/j.physletb.2026.140503.

References

[1] V.A. Kuzmin, V.A. Rubakov, M.E. Shaposhnikov, On the anomalous electroweak baryon number nonconservation in the early Universe, Phys. Lett. B 155 (1985) 36. https://doi.org/10.1016/0370-2693(85)91028-7
[2] M.E. Shaposhnikov, Structure of the high temperature gauge ground state and electroweak production of the baryon asymmetry, Nucl. Phys. B 299 (1988) 797–817. https://doi.org/10.1016/0550-3213(88)90373-2
[3] M.E. Shaposhnikov, Baryon asymmetry of the Universe in standard electroweak theory, Nucl. Phys. B 287 (1987) 757–775. https://doi.org/10.1016/0550-3213(87)90127-1
[4] M. Trodden, Electroweak baryogenesis, Rev. Mod. Phys. 71 (1999) 1463–1500. arXiv:hep-ph/9803479, https://doi.org/10.1103/RevModPhys.71.1463
[5] J.M. Cline, Baryogenesis, 2006. arXiv:hep-ph/0609145
[6] D.E. Morrissey, M.J. Ramsey-Musolf, Electroweak baryogenesis, New J. Phys. 14 (2012) 125003. arXiv:1206.2942, https://doi.org/10.1088/1367-2630/14/12/125003
[7] A.D. Sakharov, Violation of CP invariance, C asymmetry, and baryon asymmetry of the universe, Pisma Zh. Eksp. Teor. Fiz. 5 (1967) 32–35. https://doi.org/10.1070/PU1991v034n05ABEH002497
[8] A.I. Bochkarev, M.E. Shaposhnikov, Electroweak production of Baryon asymmetry and upper bounds on the Higgs and top masses, Mod. Phys. Lett. A 2 (1987) 417. https://doi.org/10.1142/S0217732387000537
[9] K. Kajantie, M. Laine, K. Rummukainen, M.E. Shaposhnikov, The electroweak phase transition: a nonperturbative analysis, Nucl. Phys. B 466 (1996) 189–258. arXiv:hep-lat/9510020, https://doi.org/10.1016/0550-3213(96)00052-1
[10] M. Laine, G. Nardini, K. Rummukainen, Lattice study of an electroweak phase transition at $m_h \simeq 126$ GeV, JCAP 01 (2013) 011. arXiv:1211.7344 [hep-ph], https://doi.org/10.1088/1475-7516/2013/01/011
[11] M.B. Gavela, P. Hernández, J. Orloff, O. Pène, Standard model CP violation and baryon asymmetry, Mod. Phys. Lett. A 9 (1994) 795–810. arXiv:hep-ph/9312215, https://doi.org/10.1142/S0217732394000629

[12] P. Huet, E. Sather, Electroweak baryogenesis and standard model CP violation, Phys. Rev. D 51 (1995) 379–394. arXiv:hep-ph/9404302, https://doi.org/10.1103/PhysRevD.51.379

[13] M.B. Gavela, P. Hernández, J. Orloff, O. Pène, C. Quimbay, Standard model CP violation and baryon asymmetry. Part 2: finite temperature, Nucl. Phys. B 430 (1994) 382–426. arXiv:hep-ph/9406289, https://doi.org/10.1016/0550-3213(94)00410-2

[14] M.J. Ramsey-Musolf, The electroweak phase transition: a collider target, JHEP 09 (2020) 179. arXiv:1912.07189 [hep-ph], https://doi.org/10.1007/JHEP09(2020)179

[15] C. Caprini, et al., Science with the space-based interferometer eLISA. II: gravitational waves from cosmological phase transitions, JCAP 04 (2016) 001. arXiv:1512.06239 [astro-ph.CO], https://doi.org/10.1088/1475-7516/2016/04/001

[16] C. Caprini, et al., Detecting gravitational waves from cosmological phase transitions with LISA: an update, JCAP 03 (2020) 024. arXiv:1910.13125 [astro-ph.CO], https://doi.org/10.1088/1475-7516/2020/03/024

[17] J. Crowder, N.J. Cornish, Beyond LISA: exploring future gravitational wave missions, Phys. Rev. D 72 (2005) 083005. arXiv:gr-qc/0506015, https://doi.org/10.1103/PhysRevD.72.083005

[18] T. Chupp, M. Ramsey-Musolf, Electric dipole moments: a global analysis, Phys. Rev. C 91 (3) (2015) 035502. arXiv:1407.1064 [hep-ph], https://doi.org/10.1103/PhysRevC.91.035502

[19] J. Engel, M.J. Ramsey-Musolf, U. van Kolck, Electric Dipole moments of nucleons, nuclei, and atoms: the standard model and beyond, Prog. Part. Nucl. Phys. 71 (2013) 21–74. arXiv:1303.2371 [nucl-th], https://doi.org/10.1016/j.ppnp.2013.03.003

[20] M. Pospelov, A. Ritz, Electric dipole moments as probes of new physics, Ann. Phys. 318 (2005) 119–169. arXiv:hep-ph/0504231, https://doi.org/10.1016/j.aop.2005.04.002

[21] J.M. Cline, M. Joyce, K. Kainulainen, Supersymmetric electroweak baryogenesis in the WKB approximation, Phys. Lett. B 417 (1998) 79–86. [Erratum: Phys. Lett. B 448, 321–321 (1999)]. arXiv:hep-ph/9708393, https://doi.org/10.1016/S0370-2693(97)01361-0

[22] T. Konstandin, Quantum transport and electroweak baryogenesis, Phys. Usp. 56 (2013) 747–771. arXiv:1302.6713 [hep-ph], https://doi.org/10.3367/UFNe.0183.201308a.0785

[23] B. Garbrecht, Why is there more matter than antimatter? Calculational methods for leptogenesis and electroweak baryogenesis, Prog. Part. Nucl. Phys. 110 (2020) 103727. arXiv:1812.02651 [hep-ph], https://doi.org/10.1016/j.ppnp.2019.103727

[24] N.F. Bell, M.J. Dolan, L.S. Friedrich, M.J. Ramsey-Musolf, R.R. Volkas, Electroweak baryogenesis with vector-like leptons and scalar singlets, JHEP 09 (2019) 012. arXiv:1903.11255 [hep-ph], https://doi.org/10.1007/JHEP09(2019)012

[25] P. Basler, L. Biermann, M. Mühlleitner, J. Müller, Electroweak baryogenesis in the CP-violating two-Higgs doublet model, Eur. Phys. J. C 83 (1) (2023) 57. arXiv:2108.03580 [hep-ph], https://doi.org/10.1140/epjc/s10052-023-11192-9

[26] K. Kainulainen, CP-violating transport theory for electroweak baryogenesis with thermal corrections, JCAP 11 (11) (2021) 042. arXiv:2108.08336 [hep-ph], https://doi.org/10.1088/1475-7516/2021/11/042

[27] J.M. Cline, B. Laurent, Electroweak baryogenesis from light fermion sources: a critical study, Phys. Rev. D 104 (8) (2021) 083507. arXiv:2108.04249 [hep-ph], https://doi.org/10.1103/PhysRevD.104.083507

[28] J.M. Cline, A. Friedlander, D.-M. He, K. Kainulainen, B. Laurent, D. Tucker-Smith, Baryogenesis and gravity waves from a UV-completed electroweak phase transition, Phys. Rev. D 103 (12) (2021) 123529. arXiv:2102.12490 [hep-ph], https://doi.org/10.1103/PhysRevD.103.123529

[29] M. Carena, M. Quirós, Y. Zhang, Electroweak baryogenesis from dark-sector CP violation, Phys. Rev. Lett. 122 (20) (2019) 201802. arXiv:1811.09719 [hep-ph], https://doi.org/10.1103/PhysRevLett.122.201802

[30] M. Carena, M. Quirós, Y. Zhang, Dark CP violation and gauged lepton or baryon number for electroweak baryogenesis, Phys. Rev. D 101 (5) (2020) 055014. arXiv:1908.04818 [hep-ph], https://doi.org/10.1103/PhysRevD.101.055014

[31] M. Carena, Y.-Y. Li, T. Ou, Y. Wang, Anatomy of the electroweak phase transition for dark sector induced baryogenesis, JHEP 02 (2023) 139. arXiv:2210.14352 [hep-ph], https://doi.org/10.1007/JHEP02(2023)139

[32] K. Enomoto, S. Kanemura, Y. Mura, Electroweak baryogenesis in aligned two Higgs doublet models, JHEP 01 (2022) 104. arXiv:2111.13079 [hep-ph], https://doi.org/10.1007/JHEP01(2022)104

[33] A. Riotto, Towards a nonequilibrium quantum field theory approach to electroweak baryogenesis, Phys. Rev. D 53 (1996) 5834–5841. arXiv:hep-ph/9510271, https://doi.org/10.1103/PhysRevD.53.5834

[34] A. Riotto, Supersymmetric electroweak baryogenesis, nonequilibrium field theory and quantum Boltzmann equations, Nucl. Phys. B 518 (1998) 339–360. arXiv:hep-ph/9712221, https://doi.org/10.1016/S0550-3213(98)00159-X

[35] C. Lee, V. Cirigliano, M.J. Ramsey-Musolf, Resonant relaxation in electroweak baryogenesis, Phys. Rev. D 71 (2005) 075010. arXiv:hep-ph/0412354, https://doi.org/10.1103/PhysRevD.71.075010

[36] V. Cirigliano, M.J. Ramsey-Musolf, S. Tulin, C. Lee, Yukawa and tri-scalar processes in electroweak baryogenesis, Phys. Rev. D 73 (2006) 115009. arXiv:hep-ph/0603058, https://doi.org/10.1103/PhysRevD.73.115009

[37] M. Postma, J. van de Vis, Source terms for electroweak baryogenesis in the vev-insertion approximation beyond leading order, JHEP 02 (2020) 090. arXiv:1910.11794 [hep-ph], https://doi.org/10.1007/JHEP02(2020)090

[38] J.M. Cline, K. Kainulainen, Electroweak baryogenesis at high bubble wall velocities, Phys. Rev. D 101 (6) (2020) 063525. arXiv:2001.00568 [hep-ph], https://doi.org/10.1103/PhysRevD.101.063525

[39] M. Postma, J. van de Vis, G. White, Resummation and cancellation of the VIA source in electroweak baryogenesis, JHEP 12 (2022) 121. arXiv:2206.01120 [hep-ph], https://doi.org/10.1007/JHEP12(2022)121

[40] V. Cirigliano, C. Lee, M.J. Ramsey-Musolf, S. Tulin, Flavored quantum Boltzmann equations, Phys. Rev. D 81 (2010) 103503. arXiv:0912.3523 [hep-ph], https://doi.org/10.1103/PhysRevD.81.103503

[41] V. Cirigliano, C. Lee, S. Tulin, Resonant flavor oscillations in electroweak baryogenesis, Phys. Rev. D 84 (2011) 056006. arXiv:1106.0747 [hep-ph], https://doi.org/10.1103/PhysRevD.84.056006

[42] H.H. Patel, M.J. Ramsey-Musolf, Stepping into electroweak symmetry breaking: phase transitions and Higgs phenomenology, Phys. Rev. D 88 (2013) 035013. arXiv:1212.5652 [hep-ph], https://doi.org/10.1103/PhysRevD.88.035013

[43] S. Inoue, G. Ovanesyan, M.J. Ramsey-Musolf, Two-step electroweak baryogenesis, Phys. Rev. D 93 (2016) 015013. arXiv:1508.05404 [hep-ph], https://doi.org/10.1103/PhysRevD.93.015013

[44] J.S. Schwinger, Brownian motion of a quantum oscillator, J. Math. Phys. 2 (1961) 407–432. https://doi.org/10.1063/1.1703727

[45] K.T. Mahanthappa, Multiple production of photons in quantum electrodynamics, Phys. Rev. 126 (1962) 329–340. https://doi.org/10.1103/PhysRev.126.329

[46] P.M. Bakshi, K.T. Mahanthappa, Expectation value formalism in quantum field theory. 1, J. Math. Phys. 4 (1963) 1–11. https://doi.org/10.1063/1.1703883

[47] P.M. Bakshi, K.T. Mahanthappa, Expectation value formalism in quantum field theory. 2, J. Math. Phys. 4 (1963) 12–16. https://doi.org/10.1063/1.1703879

[48] L.V. Keldysh, Diagram technique for nonequilibrium processes, Zh. Eksp. Teor. Fiz. 47 (1964) 1515–1527.

[49] K.-c. Chou, Z.-b. Su, B.-l. Hao, L. Yu, Equilibrium and nonequilibrium formalisms made unified, Phys. Rept. 118 (1985) 1–131. https://doi.org/10.1016/0370-1573(85)90136-X

[50] M. Dine, R.G. Leigh, P.Y. Huet, A.D. Linde, D.A. Linde, Towards the theory of the electroweak phase transition, Phys. Rev. D 46 (1992) 550–571. arXiv:hep-ph/9203203, https://doi.org/10.1103/PhysRevD.46.550

[51] G.D. Moore, Electroweak bubble wall friction: analytic results, JHEP 03 (2000) 006. arXiv:hep-ph/0001274, https://doi.org/10.1088/1126-6708/2000/03/006

[52] J.R. Espinosa, T. Konstandin, J.M. No, G. Servant, Energy budget of cosmological first-order phase transitions, JCAP 06 (2010) 028. arXiv:1004.4187 [hep-ph], https://doi.org/10.1088/1475-7516/2010/06/028

[53] D. Bodeker, G.D. Moore, Electroweak bubble wall speed limit, JCAP 05 (2017) 025. arXiv:1703.08215 [hep-ph], https://doi.org/10.1088/1475-7516/2017/05/025

[54] S. Höche, J. Kozaczuk, A.J. Long, J. Turner, Y. Wang, Towards an all-orders calculation of the electroweak bubble wall velocity, JCAP 03 (2021) 009. arXiv:2007.10343 [hep-ph], https://doi.org/10.1088/1475-7516/2021/03/009

[55] S. De Curtis, L.D. Rose, A. Guiggiani, A.G. Muyor, G. Panico, Bubble wall dynamics at the electroweak phase transition, JHEP 03 (2022) 163. arXiv:2201.08220 [hep-ph], https://doi.org/10.1007/JHEP03(2022)163

[56] B. Laurent, J.M. Cline, First principles determination of bubble wall velocity, Phys. Rev. D 106 (2) (2022) 023501. arXiv:2204.13120 [hep-ph], https://doi.org/10.1103/PhysRevD.106.023501

[57] P. Bandyopadhyay, C. Coriano, A. Costantini, Probing the hidden Higgs bosons of the $Y = 0$ triplet- and singlet-extended supersymmetric standard model at the LHC, JHEP 12 (2015) 127. arXiv:1510.06309 [hep-ph], https://doi.org/10.1007/JHEP12(2015)127

[58] P. Bandyopadhyay, C. Coriano, A. Costantini, Perspectives on a supersymmetric extension of the standard model with a Y = 0 Higgs triplet and a singlet at the LHC, JHEP 09 (2015) 045. arXiv:1506.03634 [hep-ph], https://doi.org/10.1007/JHEP09(2015)045

[59] H.H. Patel, M.J. Ramsey-Musolf, Baryon washout, electroweak phase transition, and perturbation theory, JHEP 07 (2011) 029. arXiv:1101.4665 [hep-ph], https://doi.org/10.1007/JHEP07(2011)029

[60] L. Niemi, M.J. Ramsey-Musolf, T.V.I. Tenkanen, D.J. Weir, Thermodynamics of a two-step electroweak phase transition, Phys. Rev. Lett. 126 (17) (2021) 171802. arXiv:2005.11332 [hep-ph], https://doi.org/10.1103/PhysRevLett.126.171802

[61] J.F. Gunion, H.E. Haber, The CP conserving two Higgs doublet model: the approach to the decoupling limit, Phys. Rev. D 67 (2003) 075019. arXiv:hep-ph/0207010, https://doi.org/10.1103/PhysRevD.67.075019

[62] G.C. Branco, P.M. Ferreira, L. Lavoura, M.N. Rebelo, M. Sher, J.P. Silva, Theory and phenomenology of two-Higgs-Doublet models, Phys. Rept. 516 (2012) 1–102. arXiv:1106.0034 [hep-ph], https://doi.org/10.1016/j.physrep.2012.02.002

[63] S. Inoue, M.J. Ramsey-Musolf, Y. Zhang, CP-violating phenomenology of flavor conserving two Higgs doublet models, Phys. Rev. D 89 (11) (2014) 115023. arXiv:1403.4257 [hep-ph], https://doi.org/10.1103/PhysRevD.89.115023

[64] W.H. Press, S.A. Teukolsky, W.T. Vetterling, B.P. Flannery, Numerical recipes in FORTRAN: the art of scientific computing, 2nd ed., Cambridge University Press, (1992).

[65] R. Alarcon, et al., Electric dipole moments and the search for new physics, in: Snowmass 2021, 2022. arXiv:2203.08103 [hep-ph]

[66] V. Andreev, et al., ACME, Improved limit on the electric dipole moment of the electron, Nature 562 (7727) (2018) 355–360. https://doi.org/10.1038/s41586-018-0599-8

[67] W. Altmannshofer, S. Gori, N. Hamer, H.H. Patel, Electron EDM in the complex two-Higgs doublet model, Phys. Rev. D 102 (11) (2020) 115042. arXiv:2009.01258 [hep-ph], https://doi.org/10.1103/PhysRevD.102.115042